

Analysis of Efficient Wavelet Based Volumetric Image Compression

Krishna Kumar
Department of ECE,
Motilal Nehru NIT
Allahabad, India

krishnanitald@gmail.com

Basant Kumar
Department of ECE,
Motilal Nehru NIT
Allahabad, India

singhbasant@mnnit.ac.in

Rachna Shah
Department of CSE,
NIT Kurukshetra, India

rachna.shah27@gmail.com

Abstract

Recently, the wavelet transform has emerged as a cutting edge technology, within the field of image compression research. Telemedicine, among other things, involves storage and transmission of medical images, popularly known as Teleradiology. Due to constraints on bandwidth and storage capacity, a medical image may be needed to be compressed before transmission/storage. This paper is focused on selecting the most appropriate wavelet transform for a given type of medical image compression. In this paper we have analyzed the behavior of different type of wavelet transforms with different type of medical images and identified the most appropriate wavelet transform that can perform optimum compression for a given type of medical imaging. To analyze the performance of the wavelet transform with the medical images at constant PSNR, we calculated SSIM and their respective percentage compression.

Keywords: JPEG, CT, US, MRI, ECG, Wavelet Transforms, Medical Image Compression

1. INTRODUCTION

With the steady growth of computer power, rapidly declining cost of storage and ever-increasing access to the Internet, digital acquisition of medical images has become increasingly popular in recent years. A digital image is preferable to analog formats because of its convenient sharing and distribution properties. This trend has motivated research in imaging informatics [1], which was nearly ignored by traditional computer-based medical record systems because of the large amount of data required to represent images and the difficulty of automatically analyzing images. Besides traditional X-rays and Mammography, newer image modalities such as Magnetic Resonance Imaging (MRI) and Computed Tomography (CT) can produce up to several hundred slices per patient scan. Each year, a typical hospital can produce several terabytes of digital and digitized medical images.

2. IMAGE COMPRESSION

Both JPEG and wavelet belong to the general class of “transformed based lossy compression techniques.” These techniques involved three steps: transformation, quantization, and encoding. Transformation is a lossless step in which image is transformed from the grayscale values in the special domain to coefficients in some other domain. No loss of information occurs in the transformation step. Quantization is the step in which loss of information occurs. It attempts to preserve the more important coefficients, while less important coefficients are roughly approximated, often as zero. Finally, these quantized coefficients are encoded. This is also a lossless step in which the quantized coefficients are compactly represented for efficient storage or transmission of the image [20].

2.1 JPEG Compression

The JPEG specification defines a minimal subset of the standard called baseline JPEG, which all JPEG-aware applications are required to support. This baseline uses an encoding scheme based on the Discrete Cosine Transform (DCT) to achieve compression. DCT is a generic name for a class of operations identified and published some years ago. DCT-based algorithms have since made their way into various compression methods. DCT-based encoding algorithms are always lossy by nature.

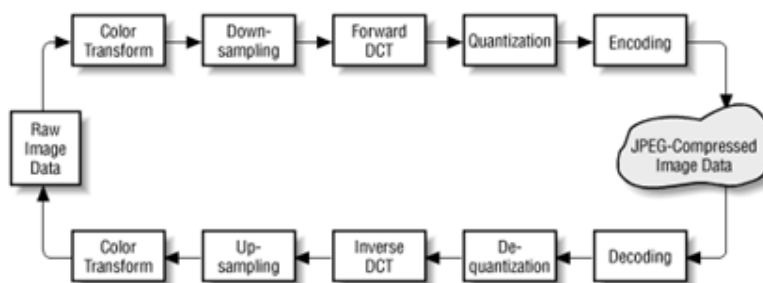


FIGURE 2.1: JPEG Compression & Decompression

2.2 Wavelet Compression

The Fourier transform is a useful tool to analyze the frequency components of the signal. However, if we take the Fourier transform over the whole time axis, we cannot tell at what instant a particular frequency rises. Short-time Fourier transform (STFT) uses a sliding window to find spectrogram, which gives the information of both time and frequency. But still another problem exists: The length of window limits the resolution in frequency. Wavelet Transform seems to be a solution to the problem above. Wavelet transforms are based on small wavelets with limited duration. The translated-version wavelets locate where we concern. Whereas the scaled version wavelets allow us to analyze the signal in different scale. It is a transform that provides the time-frequency representation simultaneously.

2.3 Decomposition Process

The image is high and low-pass filtered along the rows. The results of each filter are down-sampled by two. Each of the sub-signals is then again high and low-pass filtered, but now along the column data and the results is again down-sampled by two.

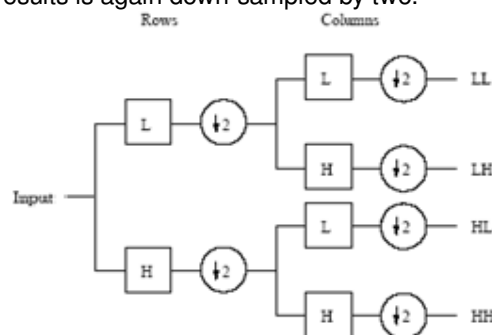


FIGURE 2.3.1: One Decomposition Step of the Two Dimensional Images

Hence, the original data is split into four sub-images each of size $N/2$ by $N/2$ and contains information from different frequency components. Fig. 2.3.2 shows the block wise representation of decomposition step.



FIGURE 2.3.2: One DWT Decomposition Step

The LL subband contains a rough description of the image and hence called the approximation subband. The HH Subband contains the high-frequency components along the diagonals. The HL and LH images result from low-pass filtering in one direction and high-pass filtering in the other direction. LH contains mostly the vertical detail information, which corresponds to horizontal edges. HL represents the horizontal detail information from the vertical edges. The subbands HL, LH and HH are called the detail subbands since they add the high-frequency detail to the approximation image.

2.4 Composition Process

Fig. 2.4 corresponds to the composition process. The four sub-images are up-sampled and then filtered with the corresponding inverse filters along the columns. The result of the last step is added together and we have the original image again, with no information loss.

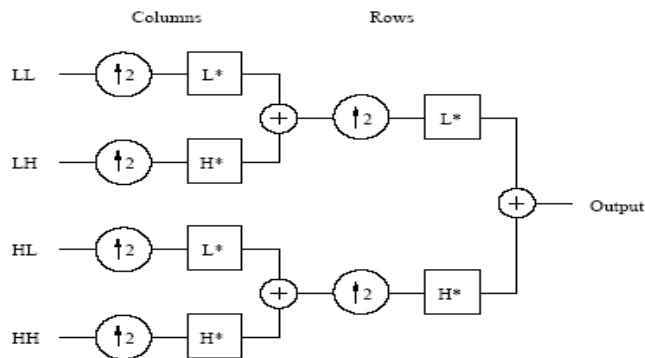


FIGURE 2.4: One Composition Step of the Four Sub Images

3. WAVELET FAMILIES

There are many members in the wavelet family, Haar wavelet is one of the oldest and simplest wavelet.

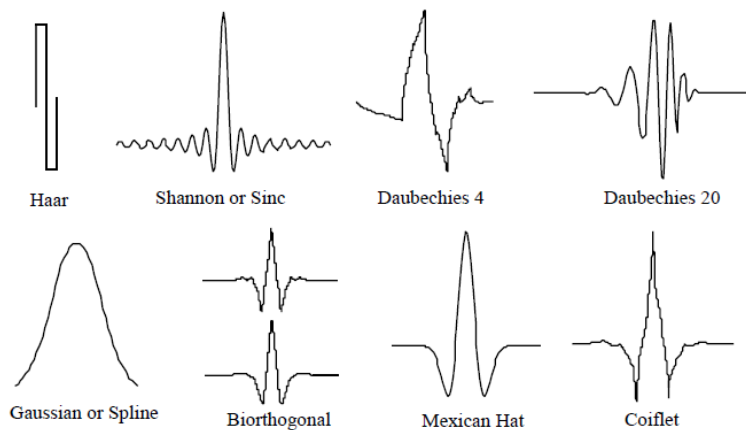


FIGURE 3: Different Types of Wavelets

Daubechies wavelets are the most popular wavelets. They represent the foundations of wavelet signal processing and are used in numerous applications. The Haar, Daubechies, Symlets and Coiflets are compactly supported orthogonal wavelets. These wavelets along with Meyer wavelets are capable of perfect reconstruction. The Meyer, Morlet and Mexican Hat wavelets are symmetric in shape. The wavelets are chosen based on their shape and their ability to analyze the signal in a particular application. Biorthogonal wavelet exhibits the property of linear phase, which is needed for signal and image reconstruction. By using two wavelets, one for decomposition (on the left side) and the other for reconstruction (on the right side) instead of the same single one, interesting properties are derived.

4. MEDICAL IMAGES

Computed tomography (CT) , is a medical imaging procedure that uses x-rays to show cross-sectional images of the body. A CT imaging system produces cross-sectional images or "slices" of areas of the body, like the slices in a loaf of bread. These cross-sectional images are used for a variety of diagnostic and therapeutic purposes. Magnetic resonance imaging (MRI) is an imaging technique used primarily in medical settings to produce high quality images of the inside of the human body. ECG (electrocardiogram) is a test that measures the electrical activity of the heart. The heart is a muscular organ that beats in rhythm to pump the blood through the body. The signals that make the heart's muscle fibres contract come from the sinoatrial node, which is the natural pacemaker of the heart. In an ECG test, the electrical impulses made while the heart is beating are recorded and usually shown on a piece of paper. Mammography can be used for diagnosis or for screening asymptomatic patients. Mammography is a highly effective imaging method for detecting, diagnosing, and managing a variety of breast diseases, especially cancer. It is an application where an emphasis on patient dose management and risk reduction is required. This is because of a combination of two factors. First, breast tissue has a relatively high sensitivity to any adverse effects of radiation, and second, mammography requires a higher exposure than other radiographic procedures to produce the required image quality. Retinal (eye fundus) images are widely used for diagnostic purposes by ophthalmologists. The normal features of eye fundus images include the optic disc, fovea and blood vessels. Ultrasound imaging is a common diagnostic medical procedure that uses high-frequency sound waves to produce dynamic images (sonograms) of organs, tissues, or blood flow inside the body.

5. FIDELITY CRITERIA

It is natural to raise the question of how much an image can be compressed and still preserve sufficient information for a given clinical application. This section discusses some parameters used to measure the trade-off between image quality and compression ratio. Compression ratio is defined as the nominal bit depth of the original image in bits per pixel (bpp) divided by the bpp necessary to store the compressed image. For each compressed and reconstructed image, an error image was calculated. From the error data, maximum absolute error (MAE), mean square error (MSE), root mean square error (RMSE), signal to noise ratio (SNR), and peak signal to noise ratio (PSNR) were calculated.

The maximum absolute error (MAE) is calculated as [21]

$$MSE = \max |f(x, y) - f^*(x, y)| \tag{5.1}$$

Where $f(x, y)$ is the original image data and $f^*(x, y)$ is the compressed image value. The formulae for calculating image matrices are:

$$MSE = \frac{1}{NM} \sum_{i=0}^{N-1} \sum_{j=0}^{M-1} [f(x, y) - f^*(x, y)] \tag{5.2}$$

$$RMSE = \sqrt{MSE} \tag{5.3}$$

$$SNR = 10 \log \left\{ \frac{\sum_{i=0}^{N-1} \sum_{j=0}^{M-1} f(x, y)^2}{\sum_{i=0}^{N-1} \sum_{j=0}^{M-1} [f(x, y) - f^*(x, y)]^2} \right\} \tag{5.4}$$

$$PSNR = 20 \log \left(\frac{255^2}{RMSE} \right) \tag{5.5}$$

Structural Similarity Index Measurement (SSIM):

Let $x, y \in R^n$ where $n > 2$. We define the following empirical quantities: the sample mean

$$\mu_x \triangleq (1/n) \sum_{i=0}^{n-1} x_i \tag{5.6}$$

The sample variance

$$\sigma_x^2 \triangleq (1/(n - 1)) (x - \mu_x)^T (x - \mu_x) = (x^T x / (n - 1)) - (n \mu_x^2 / (n - 1)) \tag{5.7}$$

and the sample cross-variance

$$\sigma_{xy} = \sigma_{yx} \triangleq \left(\frac{1}{n-1}\right) (x - \mu_x)^T (y - \mu_y) = (x^T y / (n - 1)) - (n \mu_x \mu_y / (n - 1)) \quad (5.8)$$

We define μ_x and σ_y^2 similarly. The SSIM index is defined as,

$$SSIM(x, y) \triangleq \frac{(2 \mu_x \mu_y + C_1)(2 \sigma_{xy} + C_2)}{(\mu_x^2 + \mu_y^2 + C_1)(\sigma_x^2 + \sigma_y^2 + C_2)} \quad (5.9)$$

Where $C_i > 0$, $i=1, 2$. The SSIM index ranges between -1 and 1, where positive values closed to 1 indicates a small perceptual distortion. We can define a distortion “measure” as one minus the SSIM index, that is,

$$d(x,y) \triangleq 1 - \frac{(2 \mu_x \mu_y + C_1)(2 \sigma_{xy} + C_2)}{(\mu_x^2 + \mu_y^2 + C_1)(\sigma_x^2 + \sigma_y^2 + C_2)} \quad (5.10)$$

which ranges between 0 and 2 where a value closed to 0 indicates a small distortion. The SSIM index is locally applied to $N \times N$ blocks of the image. Then, all block indexes are averaged to yield the SSIM index of the entire image. We treat each block as an n -dimensional vector where $n=N^2$.

Compression ratio, $CR = \frac{\text{number of coded bits}}{n \times m}$ where, n, m is the image size.

Percentage compression = $\frac{\text{size of original image} - \text{size of compressed image}}{\text{size of original image}} \times 100$ (5.11)

6. PROPOSED METHOD

In this proposed method we have analyzed the different medical images with different wavelet transforms at constant PSNR and computed the percentage compression and SSIM.

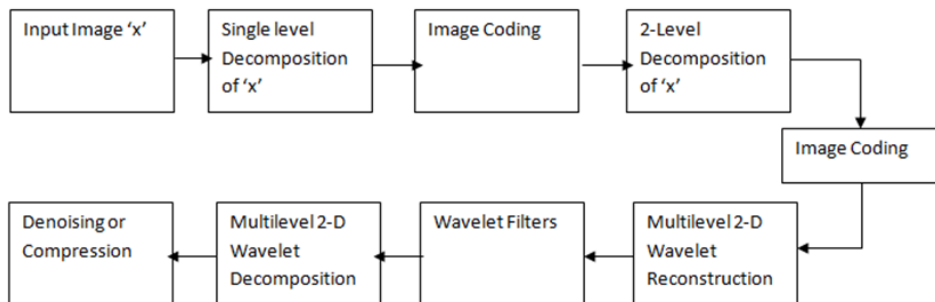


FIGURE 6: Proposed Algorithm

7. SIMULATION & RESULTS



FIGURE 7.1.1: Original images

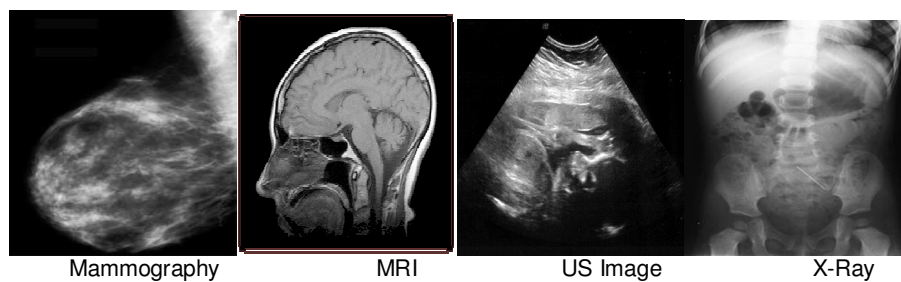


FIGURE 7.1.2: Original images

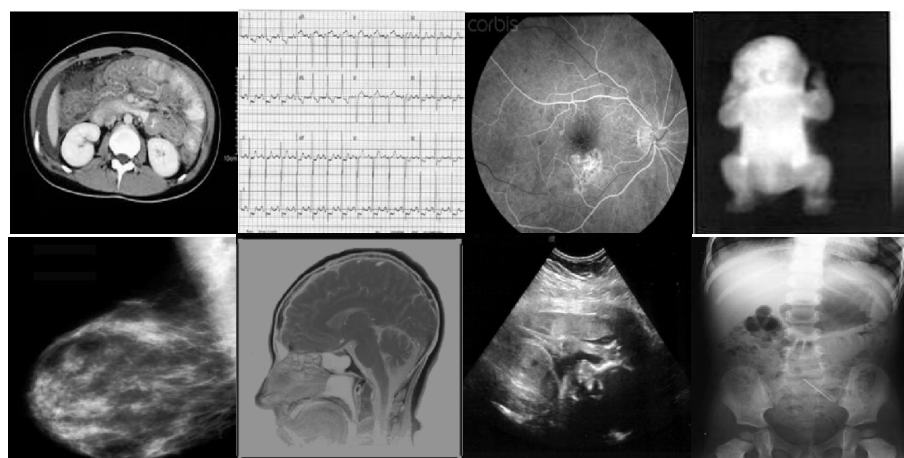


FIGURE 7.2: Compressed Images after Haar Transform at 2-Level Decomposition

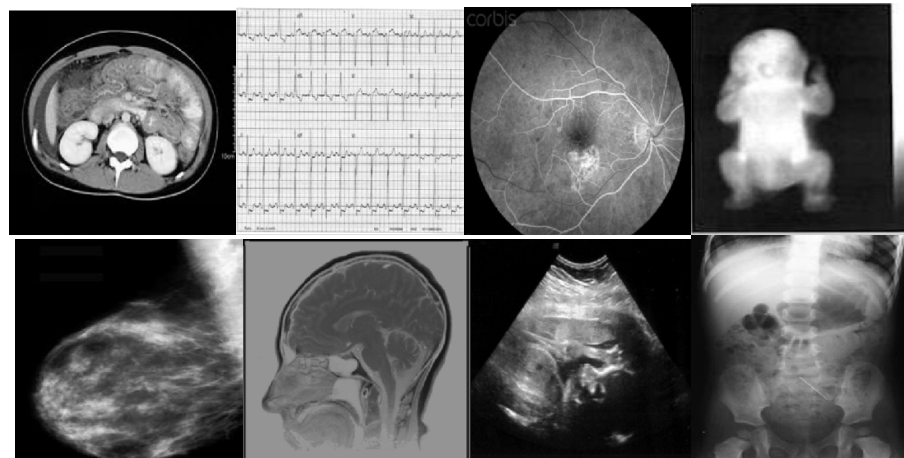


FIGURE 7.3: Compressed Images after Daubechies Transform at 2-Level Decomposition

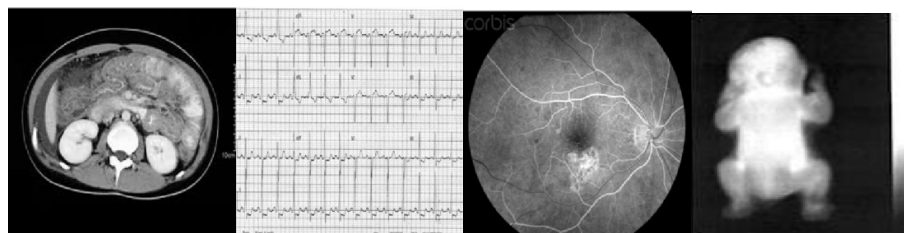


FIGURE 7.4.1: Compressed Images after Coiflets Transform at 2-Level Decomposition

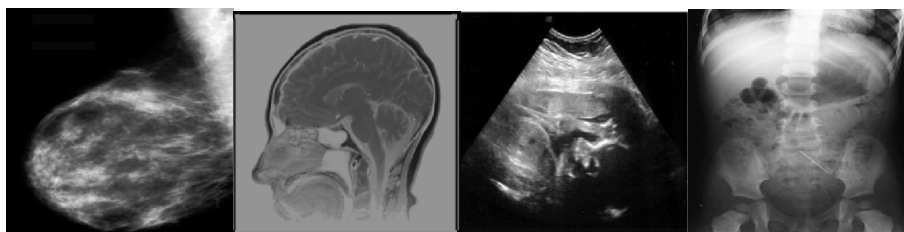


FIGURE 7.4.2: Compressed Images after Coiflets Transform at 2-Level Decomposition

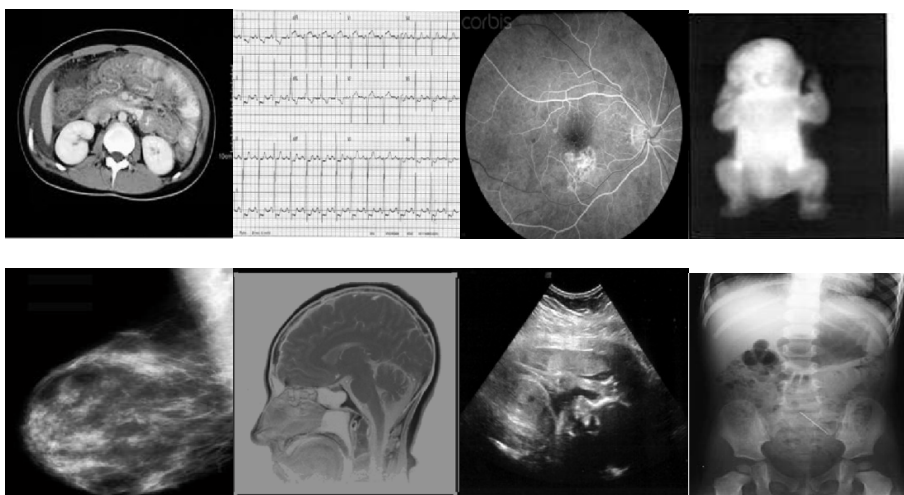


FIGURE 7.5: Compressed Images after Biorthogonal Transform at 2-Level Decomposition

Images	Wavelet Transforms			
	HAAR	Daubechie s	Biorthogon al	Coiflet s
CT	67.5415	75.4188	78.1819	80.3231
MRI	77.1469	79.6038	76.7343	74.3275
ECG	44.4733	41.0012	31.3784	30.6351
Infrared	84.2682	87.0825	85.7940	85.5303
Mammograph y	75.9598	84.5384	86.0533	86.2369
Fundus	62.4176	69.2187	68.5846	67.1999
Ultra Sound	71.2311	78.5077	79.2452	79.4678
X-Ray	78.4210	86.1492	87.0921	86.0198

TABLE 7.1: Percentage Compression for Different Medical Images with Wavelet Transforms

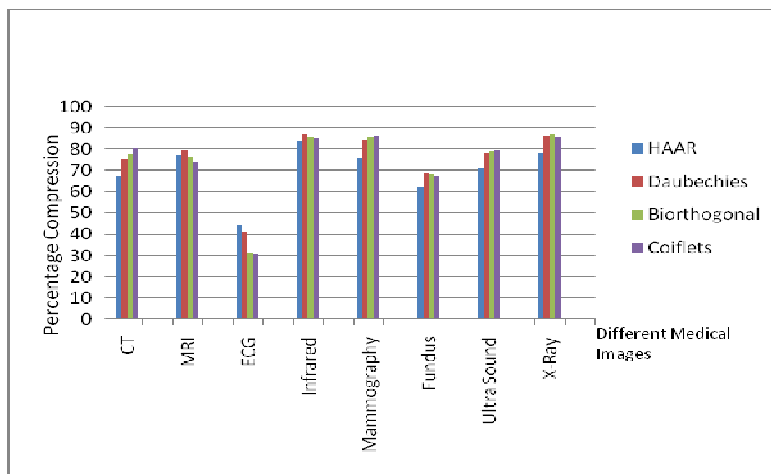


FIGURE 7.6: Percentage Compression for Different Medical Images with Wavelet Transforms

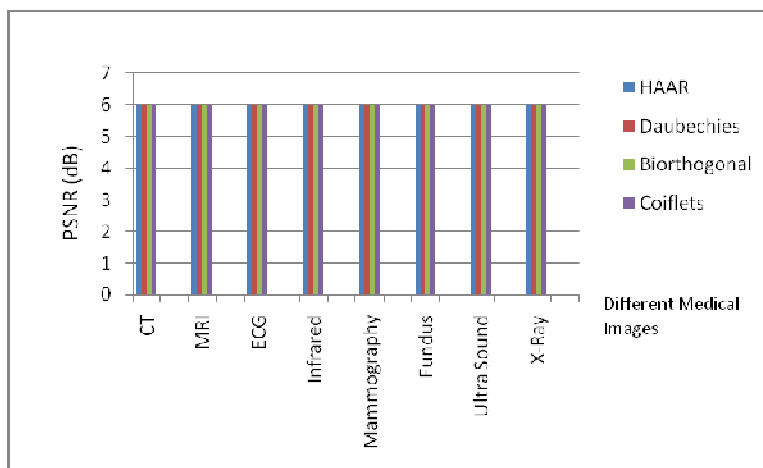


FIGURE 7.7: PSNR (dB) for Different Medical Images with Wavelet Transforms

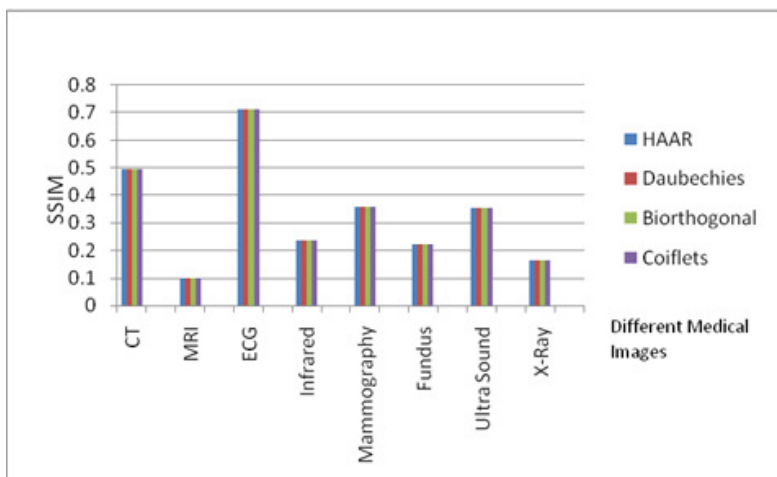


FIGURE 7.8: SSIM for Different Medical Images with Wavelet Transforms

8. CONCLUSION

In this paper we have analyzed that the Coiflets transform gives a higher percentage of compression for CT, US and Mammography images, Daubechies transform gives a higher percentage of compression for MRI, Fundus and Infrared images, Haar transform gives a higher percentage of compression for ECG images and Biorthogonal transform gives a higher percentage of compression for X-ray images at constant PSNR.

REFERENCES

- [1] Short liffe EH, Perreault LE, editors. "Medical Informatics: Computer Applications in Health Care and Biomedicine". New York: Springer, 2001.
- [2] Unser, M. and Aldroubi, A., "A review of wavelets in biomedical applications". Proc. IEEE, No. 5 1996.
- [3] Cosman, P. C., Gray, R. M., and Vetterlui, M., "Vector quantization of image subbands: A survey," IEEE Trans. Image Process. 5, No. 2, 1996.
- [4] Andrew, R. K., Stewart, B., Langer, S., and Stegbauer, K. C., "Wavelet Compression of Ultrasound Video Streams for Teleradiology". IEEE Press, New York, pp. 15–19, 1998.
- [5] Munteanu, B. A., Cristea, P., and Alexopoulos, D., "A New Quantization Algorithm for a Wavelet Compression Scheme of Coronary Angiograms". IEEE Press, New York, pp. 569–572, 1996.
- [6] Vlahakis, V. and Kitny, R. T., "Wavelet-Based Inhomogeneous, Near-Lossless Compression of Ultrasound Images of the Heart". IEEE Press, New York, pp. 549–552, 1997.
- [7] A. Said and W. A. Peralman, "An image multiresolution representation for lossless and lossy image compression," IEEE Trans. on Image Processing 5, pp. 1303-1310, Sept. 1996.
- [8] J. Luo, X.Wang, C.W.Chen, and K. J.Parker, "Volumetric medical image compression with Three- dimensional wavelet transform and octave zerotree coding," Proceedings SPIE, 1996.
- [9] A. Zandi, J. D.Allen, E. L.Schwartz, and M. Boliek, "Compression with Reversible Embedded Wavelet", RICOH California Research Center Report, 1997.
- [10] A. Bilgin and M.W.Marcellin, "Efficient lossless coding of medical image volumes using reversible integer wavelet transforms in Image Processing", Proc. of Data Compression Conference , March 1998.
- [11] Z. Xiong, X. Wu, and D. Y.Yun, "Progressive coding of medical volumetric data using 3-D integer wavelet packet transform," in Image Processing, IEEE Workshop on Multimedia Signal Process- ing , pp. 553-558, Dec. 1998.
- [12] M.Vetterli and J.Kovacevic, "Wavelets and Subband Coding", Prentice Hall, Inc, 1995.
- [13] A. Said and W. A. Pearlman, "Reversible image compression via multiresolution representation and predictive coding," in Visual Communications and Image Processing '93, Proc. SPIE, pp.664- 674, Nov.1993.
- [14] Wang, J. and Huwang, H. H., "Medical image compression by using three dimensional wavelet Transformation". IEEE Trans. Medical Imaging 15, No. 4 ,1996.
- [15] Winger, L. L. and Ventsanopoulism, A. N., "In Birthogonal Modified Coiflet Filter for Image Comp-ression". IEEE Press, New York, pp. 2681–2684, 1998.
- [16] Manuca, "Medical image compression with set partitioning in hierarchical trees". In Proceedings of the 18th Annual International Conference of the IEEE Engineering in Medicine and Biology Society, Amsterdam, pp. 1224–1225, 1996.

- [17] J. I. Koo, H. S. Lee, and Y. Kim, "Applications of 2-D and 3-D compression algorithms to Ultrasound images," SPIE Image Capture, Formatting, and Display, vol. 1653, pp. 434-439, 1992.
- [18] H. Lee, Y. Kim, A. H. Rowberg, and E. A. Riskin, "Statistical distributions of DCT coefficients and their application to an interframe compression algorithm for 3d medical images," IEEE Trans. Med. Imag., vol. 12, no. 3, pp. 478-485, Sept. 1993.
- [19] K. K. Chan, C. C. Lau, S. L. Lou, A. Hayrapetian, B. K. T. Ho, and H. K. Huang, "Three Dimensional transform compression of images from dynamic studies," SPIE med. Imag. IV: Image Capture and Display, vol. 1232, pp. 322-326, 1990.
- [20] Bradley J. Erickson, Armando Manduca, "Wavelet compression of medical images," Journal of Radiology, vol. 206, pp. 599-607, 1998.
- [21] K Stephen & J.D.Thomson, "Performance analysis of a new semiorthogonal spline wavelet Compression algorithm for medical images," Med. Phy., vol. 27, pp. 276-288, 2000.
- [22] Brammer MJ. "Multidimensional wavelet analysis of functional magnetic resonance images". Hum Brain Mapp. 6(5-6):378-82, 1998.
- [23] DeVore RA, Jawerth B, Lucier BJ. "Image compression through wavelet transforms coding". IEEE Trans. on Information Theory, 38:719-46, 1992.
- [24] A. Munteanu et al., "Performance evaluation of the wavelet based techniques used in the lossless and lossy compression of medical and preprint images", IRIS, TR-0046, 1997.
- [25] N.J. Jayant, P. Noll, "Digital Coding of Waveforms", Prentice-Hall, Englewood Cliffs, NJ, 1984.
- [26] J.S. Taur, and C.W. Tao, "Medical Image Compression using Principal Component Analysis," International Conference on Image Processing, Volume: 1, pp: 903 -906, 1996.